

## CARBON ABUNDANCES IN RED GIANT STARS IN THE GLOBULAR CLUSTERS M92 AND NGC 6397

R. A. BELL

University of Maryland

R. J. DICKENS

Royal Greenwich Observatory

AND

B. GUSTAFSSON

Uppsala Universitets Astronomiska Observatorium

Received 1978 August 23; accepted 1978 November 1

### ABSTRACT

Model atmospheres for globular cluster stars have been used to compute synthetic spectra for the wavelength regions 3500–4350 Å and 1.9 to 2.5  $\mu\text{m}$ . These calculations have been carried out for various carbon, nitrogen, and oxygen abundances. The spectra in the G-band region have been compared with medium- and high-dispersion spectra of six red giant and asymptotic giant branch stars in the two very metal poor globular clusters M92 and NGC 6397. The temperatures and gravities of the stars have been found from synthetic colors and absolute magnitudes. The comparison suggests that all of the stars are carbon deficient relative to iron, by a factor of up to 10. Departures from LTE are unlikely to contribute very significantly to these deficiencies. The low carbon abundance is supported by analysis of the infrared CO indices of the two M92 stars. The synthetic spectra have also been used to compute the effect of changes in carbon abundance on DDO colors. The  $[C(42 - 45), C(45 - 48)]$ -diagram suggests that the carbon weakness first occurs for stars brighter than about  $M_v = -0.7$ , in good agreement with the results of stellar model calculations by Sweigart and Mengel. Unfortunately, the stellar CN effects on DDO colors are too small to be used to determine nitrogen abundances.

*Subject headings:* clusters: globular — spectrophotometry — stars: abundances — stars: late-type

### I. INTRODUCTION

The abundances of the CNO elements in globular cluster giant stars are of great interest because either they relate directly to the question of the occurrence, location, and extent of envelope mixing during red giant evolution or, if mixing does not occur, they relate directly to the early production of elements in the Galaxy. Because of this, some information about the CNO abundances in horizontal-branch and asymptotic-branch stars should result in progress in understanding further these later stages of evolution in globular clusters.

The subject has attracted considerable attention in recent years with the recognition of anomalies in observed globular cluster spectra and photometric color indices for globular cluster stars and with theoretical attempts to predict atmospheric abundance anomalies by various kinds of mixing in evolving stellar models. Until now, these attempts have been largely unsuccessful (see Sweigart and Mengel 1979 for a brief review). On the observational side, particular attention should be drawn to the apparently anomalous weaknesses of the G band in spectra of stars in several clusters (Zinn 1973; Butler, Carbon, and Kraft 1975; Norris and Zinn 1977), the anomalous strengths of

CN in the spectra of some stars in the globular cluster  $\omega$  Cen (Dickens and Bell 1976; Bessell and Norris 1976) and in other clusters (e.g., Bell, Dickens, and Gustafsson 1975), and the existence of “carbon” stars in  $\omega$  Cen (Harding 1964; Dickens 1972; Bond 1975). Quantitative analyses showing that the enhancements of CH and CN are indeed caused by overabundances of carbon and nitrogen in the anomalous  $\omega$  Cen stars have been carried out by Bell and Dickens (1974) and Dickens and Bell (1976). In the case of the carbon stars, where CH and CN are greatly enhanced and  $C_2$  is strong, the dominant effects probably relate to late evolutionary phases; but in the other stars, the smaller anomalies in the strengths of CN and CH (including weakening of the G band) could well arise during the star’s first ascent of the giant branch, or, as mentioned above, could be of much earlier origin.

There is the further possibility, studied in this paper, that some such peculiarities may be only apparent, being due entirely or partly to non-LTE effects in spectral line formation.

We have mentioned the considerable variation in the strength of the G band among stars in several globular clusters. This is of particular interest now in view of the recent theoretical possibility discussed by Sweigart and Mengel (1979) that carbon depletion can indeed

be expected to arise in a globular cluster giant star through a mechanism involving mixing by meridional circulation currents driven by core rotation in the star. We therefore concentrate our attention in this paper on quantitative determination of the carbon abundances through study of the CH lines. The work forms

part of a continuing program of abundance determinations in globular cluster stars using synthetic spectrum analysis. We have investigated the carbon abundance using medium- to high-dispersion spectra in four globular clusters: M92, NGC 6397, M13, and NGC 6752. This paper presents the results for the most

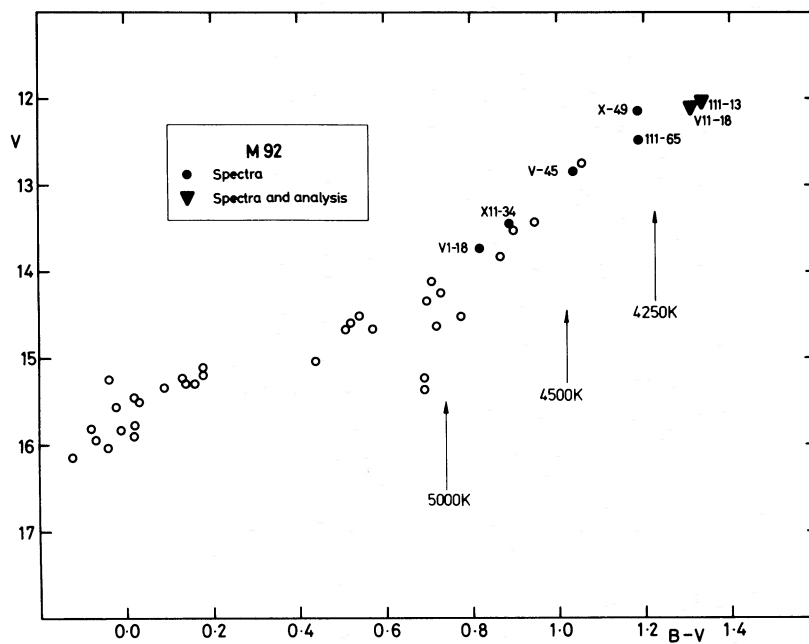


FIG. 1a

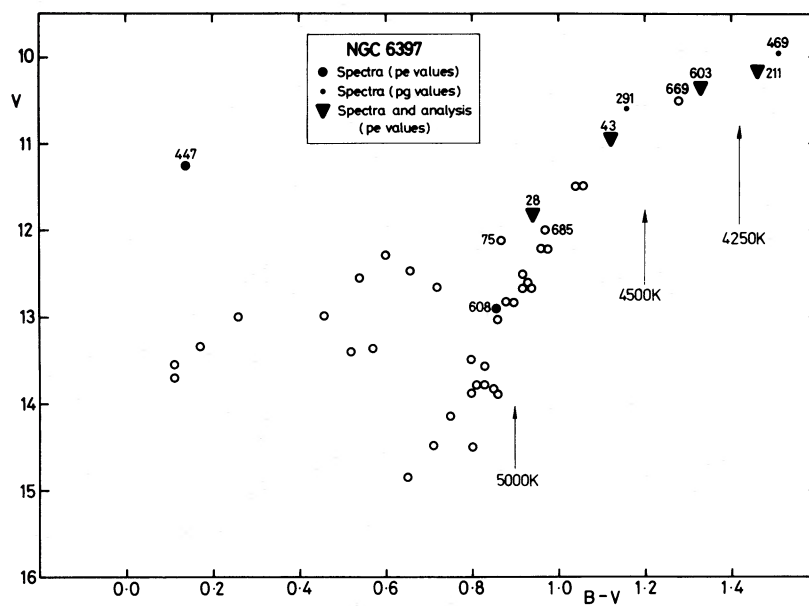


FIG. 1b

FIG. 1.—Representative color-magnitude diagrams (a) for M92 from photoelectric data by Sandage and Walker and (b) for NGC 6397 from mostly photoelectric data by Cannon. The labeled filled symbols denote stars for which we have spectra available, with the stars analyzed in detail shown as triangles.

metal-poor of these clusters, i.e., M92 and NGC 6397 ( $[\text{Fe}/\text{H}] \sim -2.0$ ). A later paper will discuss the other two, more metal-rich clusters, M13 and NGC 6752.

## II. OBSERVATIONS

Figure 1a shows a representative color-magnitude diagram of M92, plotted using photoelectric data from Table 1 of Sandage and Walker (1966). Figure 1b shows a similarly representative diagram for NGC 6397, based almost entirely on the photoelectric data given by Cannon (1974). In both diagrams, filled symbols denote the stars for which we have spectra available, with identification numbers as used in the sources quoted above. Stars with spectra which have been analyzed in detail and are discussed in this paper are shown as triangles. In the case of M92, they include only the brightest red giants whereas the NGC 6397 sample contains one asymptotic giant branch star (RGO 28) and possibly another (RGO 43), as well as two brighter red giant stars.

The spectra of the stars in M92 have been generously provided by the Hale Observatories and are part of a collection of Palomar (200 inch) coude spectra of globular cluster giant stars obtained by A. J. Deutsch, J. L. Greenstein, and O. C. Wilson and are currently on loan to one of us (R. J. D.). The plates used in the present study have a reciprocal dispersion of  $18 \text{ \AA mm}^{-1}$  and cover the wavelength interval  $4000\text{--}4950 \text{ \AA}$ . The plates used for the star III-13 are the same as those used by Helfer, Wallerstein, and Greenstein (1959) in their original analysis.

The spectra of the NGC 6397 stars were obtained with an image-tube spectrograph on the Radcliffe 74 inch (1.9 m) telescope at times between 1971 and 1973 using Carnegie (with Ila-O emulsion) and spectrotracon (with G5 emulsion) image tubes at nominal reciprocal dispersions of 22.5, 50, and  $150 \text{ \AA mm}^{-1}$ . Only the 22.5 and  $50 \text{ \AA mm}^{-1}$  material has been used in the present analysis. The spectra have projected slit widths of 12.5 and  $20 \mu\text{m}$  and cover the wavelength regions  $3790\text{--}4365 \text{ \AA}$  and  $3750\text{--}4900 \text{ \AA}$ , respectively.

Tracings of the spectra were made using a PDS microphotometer with a  $5 \mu\text{m}$  slit and digital recording. After being converted to an intensity scale, the spectra were smoothed using a least squares procedure (Savitsky and Golay 1964) and plotted with wavelength scales of  $0.2$  and  $0.5 \text{ \AA mm}^{-1}$  for detailed comparison with theoretical spectra.

In the subsequent analysis, we shall also make use of infrared narrow-band observations in M92 by Cohen, Frogel, and Persson (1978). They measured the first overtone bands of CO using filters centered at  $2.20$  and  $2.36 \mu\text{m}$  with half-widths of  $0.11$  and  $0.08 \mu\text{m}$ , respectively. In addition, observations on the DDO system by Norris and Zinn (1977) and Hesser, Hartwick, and McClure (1977) of stars in M92, and from Bessell and Norris (1978) for stars in NGC 6397, will be discussed.

## III. ANALYSES OF STELLAR SPECTRA

Bell *et al.* (1976) have published an extensive grid of flux-constant model atmospheres for cool stars. These

models include the effects of line blanketing and convection. Bell and Gustafsson (1978) have computed synthetic spectra for many of the models of this grid and have used these spectra to compute synthetic colors. Gustafsson and Bell (1978) give an extensive discussion of the accuracy of the colors. On the basis of this discussion, the observed  $B - V$  colors can be used to yield stellar temperatures when the surface gravity and chemical composition are known. The surface gravities can be obtained from the absolute magnitudes. The overall chemical compositions have been obtained from previous abundance determinations of individual cluster stars, combined with estimates from our computed and observed spectra and, in the case of NGC 6397, the properties of its color-magnitude diagram (Butler 1975). We find  $[\text{Fe}/\text{H}] = -2.3$  for M92 and  $-2.0$  for NGC 6397, with probable uncertainties of about  $\pm 0.3$ . We have adopted  $[\text{Fe}/\text{H}] = -2.0$  for both clusters but give in the later discussion the effects of changes in these values on the results.

Using reddening corrected distance moduli of  $(V_0 - M_v) = 14.1$  and  $11.8$  for M92 and NGC 6397, respectively, and  $E(B - V) = 0.02$  and  $0.18$  (Sandage 1970; Cannon 1974),  $M_v$  and  $(B - V)_0$  values can be found from the  $V$  and  $B - V$  data of Sandage and Walker (1966) and Cannon. The values for our stars are given in Table 1. Throughout the paper all colors used have been corrected for reddening.

Assuming a mass of  $0.8 M_\odot$  for globular cluster giants, we can compute  $M_{\text{bol}}$  for the grid models from the equation  $M_{\text{bol}} = 4.72 + 2.5[\log g - 10(T_{\text{eff}}) - 2.5[M]]$ , where  $[X] = \log X_* - \log X_\odot$ ,  $g$  = surface gravity,  $T_{\text{eff}}$  = effective temperature and  $M$  = mass. Then, using the bolometric corrections and  $B - V$  colors of Bell and Gustafsson (1978), we find the  $(M_v, B - V)$ -diagram of the models. This diagram is shown as Figure 2 for the relevant range of  $T_{\text{eff}}$ ,  $\log g$ , with our stars also plotted. On the basis of their positions, we adopted the values of  $T_{\text{eff}}$  and  $\log g$  given in Table 1. When these parameters differed significantly from the values of the grid models, we used our program MARCS to generate new model atmospheres. These models were computed in exactly the same manner as the grid models, following the methods described by Gustafsson *et al.* (1975). The adopted model parameters for all stars are given in Table 1.

TABLE 1  
OBSERVATIONAL DATA AND ATMOSPHERIC PARAMETERS

Object	$(B - V)_0$	$M_v$	$T_{\text{eff}}$	$\log g$	Model Used
M92:					
III-13...	1.31	-2.1	4200	0.8	4250/0.75/-2.0
VII-18...	1.29	-2.0	4250	0.9	4250/0.75/-2.0
NGC 6397:					
28.....	0.76	-0.5	4950	2.0	5000/2.25/-2.0
43.....	0.94	-1.4	4600	1.5	4600/1.50/-2.0
603.....	1.15	-2.0	4400	1.0	4400/1.00/-2.0
211.....	1.28	-2.2	4250	0.8	4250/0.75/-2.0

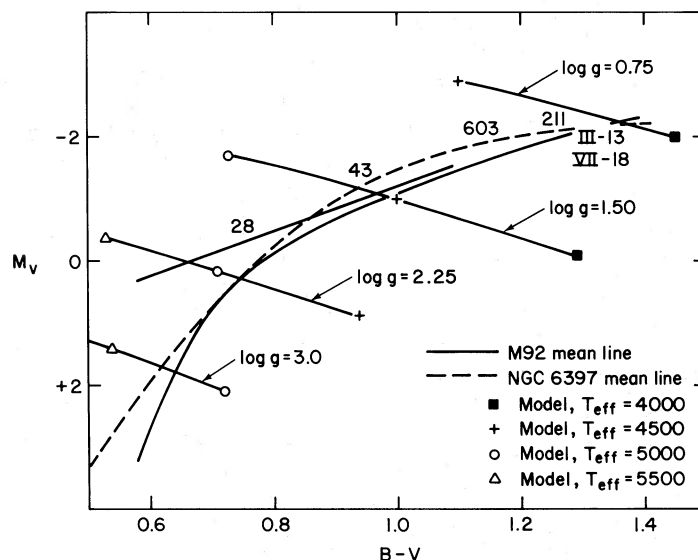


FIG. 2.—The  $(M_v, B - V)$ -values of the Bell *et al.* (1976) models for  $[A/H] = -2.0$ , calculated according to the description in the text and references cited therein, are plotted, together with the corresponding values for the NGC 6397 stars 28, 43, 211, and 603 and the M92 stars III-13 and VII-18.

Gustafsson and Bell (1978) have shown that the model 4500/1.5/-2.0 gives a good fit to the spectral scan of the M92 star XII-8 given in Christensen (1972), indicating a  $T_{\text{eff}}$  close to 4500 K. The  $M_v$  and  $B - V$  of this star are  $-1.4$  and  $1.04$ , respectively, and therefore we obtain  $T_{\text{eff}} = 4450$  K from Figure 2, in close agreement with the scanner result. We have also found that if our theoretical calibration of  $(R - I)_K$  (instead of  $B - V$ ) is used, consistent effective temperatures are obtained for the cluster stars (cf. Gustafsson and Bell 1978).

The techniques which have been used to compute synthetic stellar spectra have been exhaustively described by Bell and Gustafsson (1978). Questions of the adequacy of the LTE assumption, neglect of sphericity effects, and other assumptions will be examined at the end of this section. The values adopted for the logarithmic abundances of CNO in the Sun are 8.62, 8.00, and 8.86, respectively. The value of  $f_{00}$  for CH and CN lines was found by fitting solar spectra computed using these abundances and the Harvard Smithsonian Reference Atmosphere (HSRA, Gingerich *et al.* 1971) to the Kitt Peak Preliminary Solar Atlas (Brault and Testerman 1972). Previous calculations by Bell and Gustafsson (1978) gave lines of the (0, 0) sequence of the violet CN bands which were too strong whereas the (0, 1) lines were satisfactory, an effect noted earlier by Grevesse and Sauval (1973). The physical cause of this is unknown. For the current work,  $f_{00}$  for CN was reduced by a factor of 2 to 0.0331, so that lines of the (0, 0) sequence would be computed to have the right strength in the solar spectrum, and the line absorption coefficients of lines of the (0, 1) sequence were doubled, an artifact which keeps them at the correct strength in the computed solar spectrum. The recent analysis of solar CNO

abundances by Lambert (1978) suggests uncertainties of  $\pm 0.1$  dex. This suggests an uncertainty of, say,  $\pm 0.2$  in the values of  $[C/A]$ <sup>1</sup> deduced for the globular cluster stars, the uncertainty arising from uncertainty in the solar abundances and the value of  $f_{00}$  for CH.

One improvement made over the work of Bell and Gustafsson (1978) is a further check of the adequacy of the atomic and molecular line data. Since only a relatively small wavelength region is being studied, it is feasible to compute detailed synthetic spectra for comparison with the Kitt Peak Atlas; this enabled us to carry out a more detailed fit than was possible using previous solar atlases. The HSRA was again used to compute synthetic spectra at the center of the solar disk for the wavelength region 4000–4350 Å. On the basis of this comparison, the line data were then changed in the following way to obtain better agreement between theory and observation. The oscillator strengths of 47 atomic lines were altered, and the wavelengths of 7 CH lines were also changed. These wavelength changes are particularly necessary near band heads, such as the Q-branch head of the (2, 2) band at 4323 Å. As a check, a synthetic spectrum was then also computed for Arcturus, using the model 4200/1.5/-0.5, the notation being  $T_{\text{eff}}/\log g/[A/H]$ . A comparison of this spectrum and the Arcturus Atlas (Griffin 1968) is given in Figure 3 for selected wavelength regions and shows generally satisfactory agreement. These regions are used in subsequent analyses of our stars.

<sup>1</sup> We use A to denote all elements except for H and He and, in cases like the present one, the element or elements being discussed.  $[C/A] = -1.0$  means the carbon abundance has been reduced by a factor of 10 in the calculations.

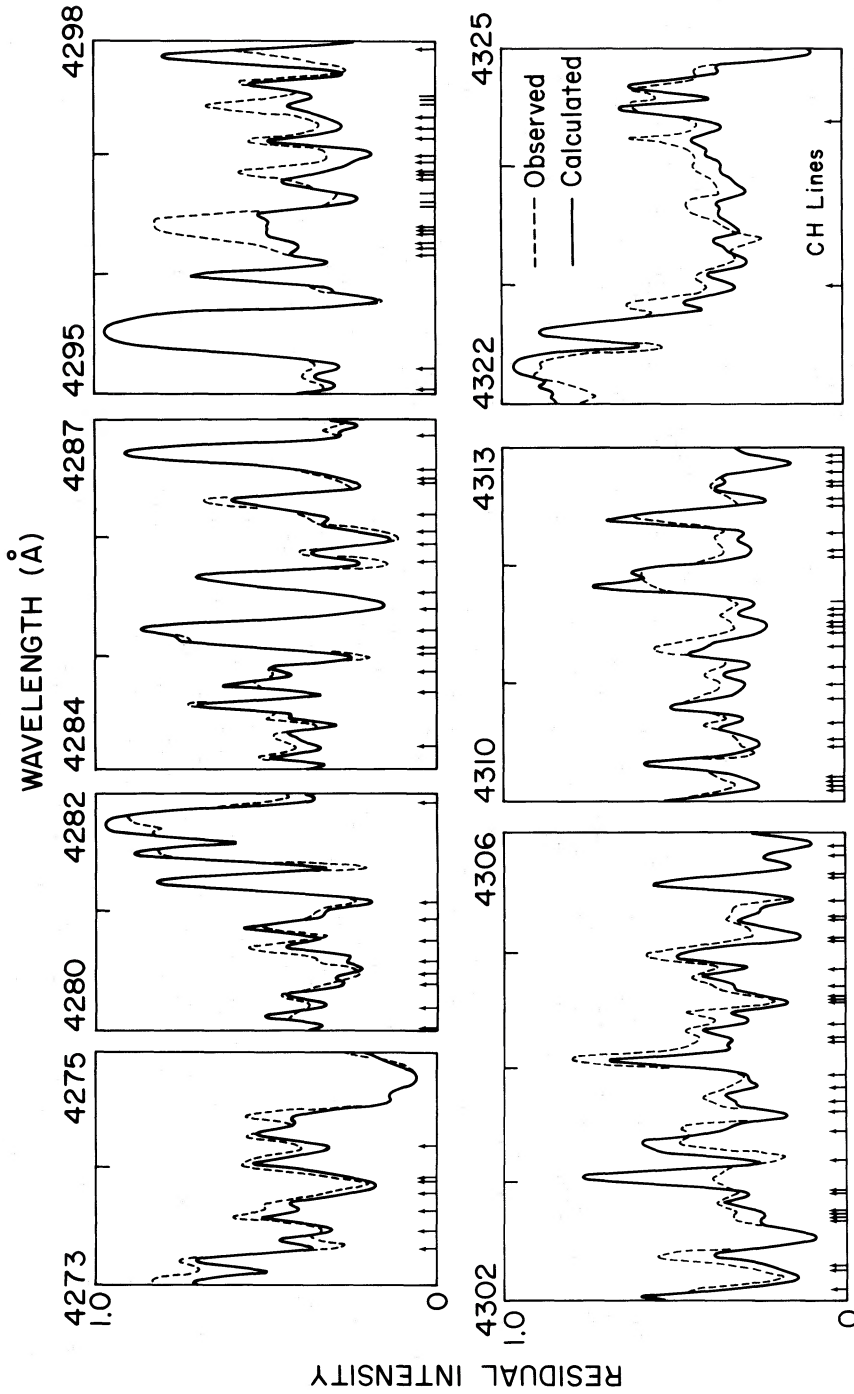


FIG. 3.—The observed spectrum (*dashed line*) of Arcturus (Griffin 1968) is compared with a synthetic spectrum (*solid line*) in the various wavelength regions used to determine CH abundances in the globular cluster stars. The wavelengths of CH lines are indicated. The lines are so numerous between 4323.0 and 4324.4 Å that they cannot be individually marked.

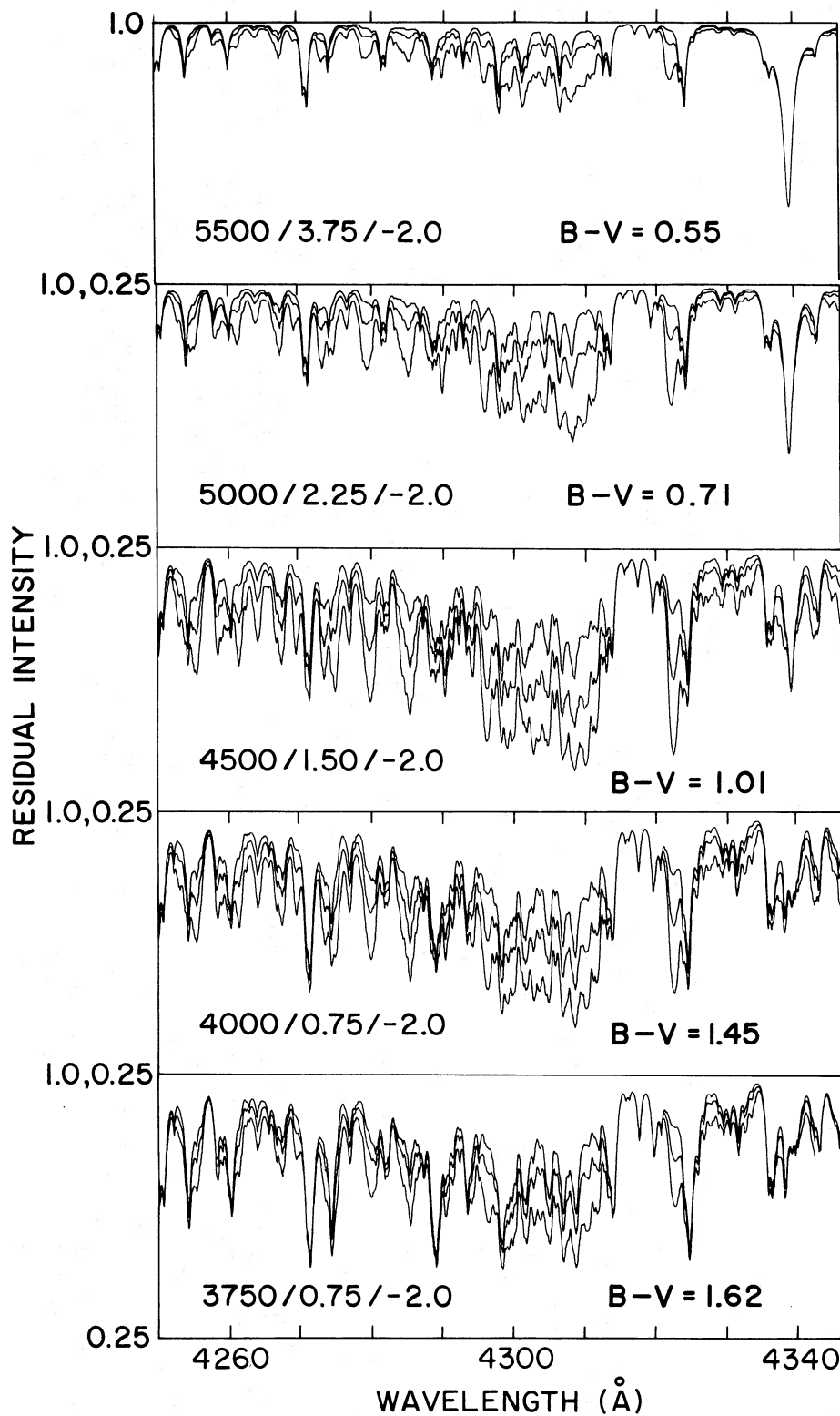


FIG. 4.—Theoretical spectra are shown for models which approximately correspond to various points along the giant branch of a globular cluster with  $[A/H] = -2.0$ . The spectrum of each model has been computed for carbon abundances of  $[C/A] = 0, -0.5,$  and  $-1.0$ , and the effects of these differences are readily apparent for  $T_{\text{eff}}$  of 5000 K or cooler. The  $B - V$  colors are indicated. To save space, the residual intensity (vertical) scale goes between 0.25 and 1.0.

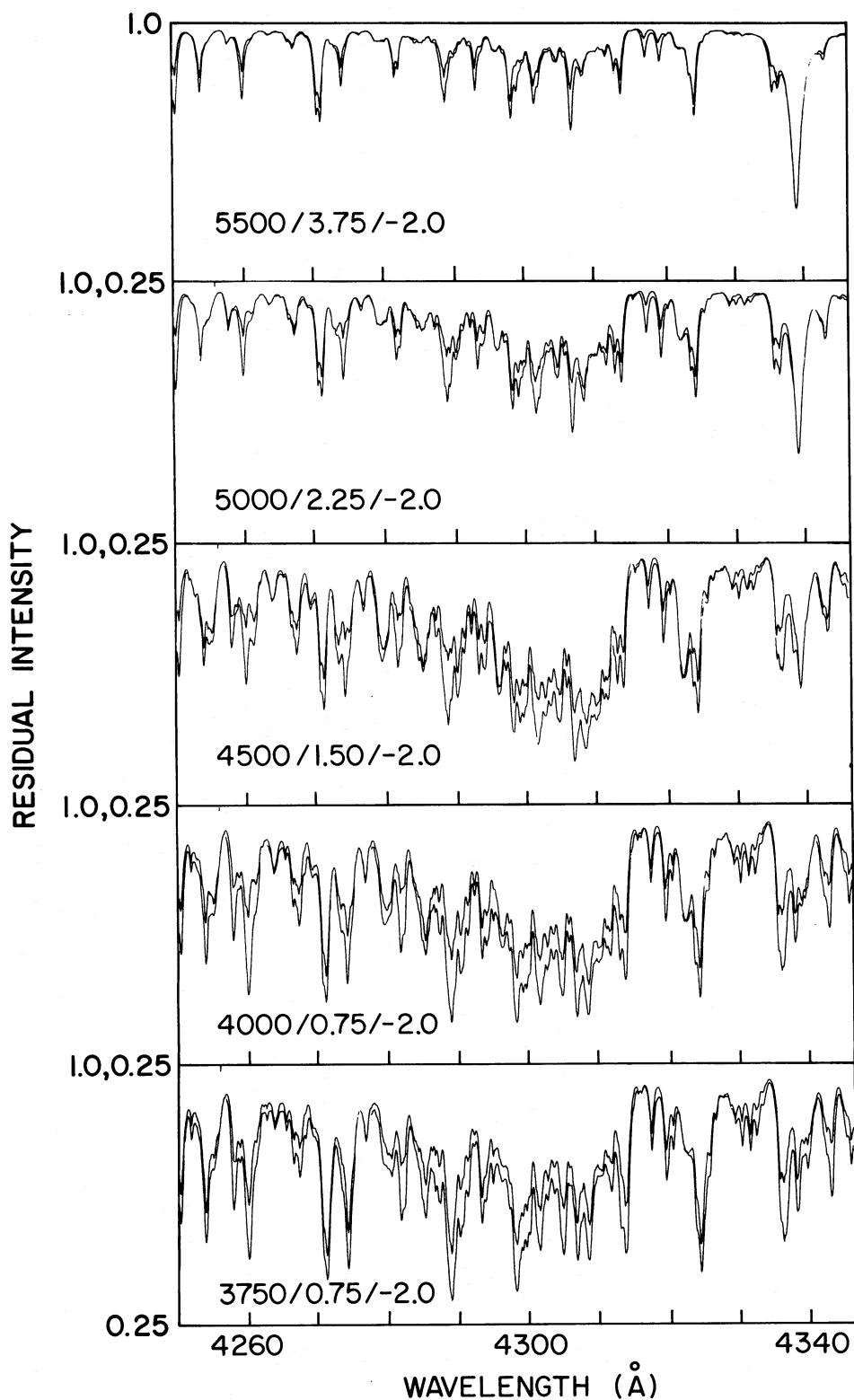


FIG. 5.—Theoretical spectra for models which approximately correspond to various points along the giant branch of a globular cluster with  $[A/H] = -2.0$ , illustrating the effects of changing the DBV from 2 to 4  $\text{km s}^{-1}$  in models with  $[C/A] = -0.5$ . The residual intensity (vertical) scale goes between 0.25 and 1.0.

One further improvement made to the synthetic spectrum program lay in the treatment of damping. At the low pressures in the atmospheres of globular cluster giants, the damping is primarily natural. In previous work, a constant value of  $\Gamma_{\text{nat}} = 1.13 \times 10^8$  was used for all lines except Ca II H and K. In the present work, values of  $\Gamma_{\text{nat}}$  were found from Einstein  $A$ -values for the strong lines  $\lambda\lambda 4250.79, 4271.76, 4282.41, 4294.13, \text{ and } 4325.76$  of Fe I,  $\lambda 4254.35$  of Cr I, and  $\lambda 4307.91$  of Cr II.

In order to test the resolution necessary in synthetic spectrum calculations for the present project, spectra were calculated for the model  $4250/0.75/-2.0$  using steps of, first,  $0.02 \text{ \AA}$  and, second,  $0.10 \text{ \AA}$  between each successive flux calculation. Following convolution with an instrumental profile of the form  $\exp(-|\Delta\lambda|/0.2)$ , comparison of these spectra showed only very small differences, and a step size of  $0.1 \text{ \AA}$  was consequently used for all successive spectrum calculations, with the exception of the search for  $^{13}\text{CH}$  features where the higher resolution was used.

In order to examine the problem of weak G band stars in general, an atlas of theoretical globular cluster stellar spectra was prepared. The grid models  $5500/3.75/-2, 5000/2.25/-2, 4500/1.5/-2, 4000/0.75/-2,$  and  $3750/0.75/-2$  were used for this atlas in order to represent the giant branch of a cluster with  $[A/H] = -2.0$  for  $0.5 \leq B - V \leq 1.5$ . The calculations were carried out for four different cases, viz., (a) the standard case with all abundances equal to 0.01 of their solar value and a Doppler broadening velocity (DBV) equal to  $2 \text{ km s}^{-1}$ , representing both thermal and microturbulent terms for iron atoms; (b) as (a) except that  $[C/A] = -0.5$ ; (c) as (a) except that  $[C/A] = -1.0$ ; (d) as (a) except that  $\text{DBV} = 4 \text{ km s}^{-1}$ . Note that DBV for CH is typically  $2.9 \text{ km s}^{-1}$  when  $\text{DBV} = 2 \text{ km s}^{-1}$  for iron, owing to the greater

thermal contribution in the former case. The calculations covered the wavelength range  $4050\text{--}4350 \text{ \AA}$ . The wavelength region  $4250\text{--}4350 \text{ \AA}$  of these spectra is shown in Figure 4 where cases (a), (b), and (c) have been overlaid, and in Figure 5 where (a) and (d) have been overlaid. The spectra have been convolved with the instrumental profile  $\exp(-|\Delta\lambda|/0.4)$  and should resemble  $50 \text{ \AA mm}^{-1}$  photographic or electronographic image-tube spectra.

The atlas shows the temperatures at which the G band is intrinsically weak. It also indicates which are the best spectral features to use to determine the carbon depletion. On the basis of Figure 4, the seven wavelength regions selected for determination of  $[C/A]$  values are:  $4273\text{--}4275 \text{ \AA}, 4280\text{--}4282 \text{ \AA}, 4285\text{--}4287 \text{ \AA}, 4296\text{--}4298 \text{ \AA}, 4302\text{--}4305 \text{ \AA}, 4310\text{--}4313 \text{ \AA},$  and  $4322\text{--}4324 \text{ \AA}$ . The first region was used only in the higher-dispersion Palomar spectra.

Figure 4 shows the temperature sensitivity of the G band and CH features. At  $T_{\text{eff}} = 5500 \text{ K}$  ( $B - V = 0.5$ ) it would be difficult to see any weakness of CH features caused by carbon abundance changes whereas at  $T_{\text{eff}} = 5000 \text{ K}$  ( $B - V = 0.7$ ) it appears that deficiencies of up to  $[C/A] = -0.5$  could be measured. The CH lines reach maximum strength at  $4500 \text{ K}$  ( $B - V = 1.0$ ), and changes with  $[C/A]$  in many CH features can be clearly seen. At this temperature and at  $T_{\text{eff}} = 4000 \text{ K}$  ( $B - V = 1.4$ ) it is possible to determine carbon deficiencies of up to  $[C/A] = -1.0$  or even more. The CH lines are weaker at  $3750 \text{ K}$ , and it may not be possible to conclude that  $[C/A] \leq -0.5$  in a star of this temperature.

The effect of changes in DBV are shown in Figure 5. It is noticeable that some features are little affected whereas others are affected much more (compare the features at  $4285 \text{ \AA}$  and  $4289 \text{ \AA}$ ). While it does appear that uncertainties in the value for DBV will affect the

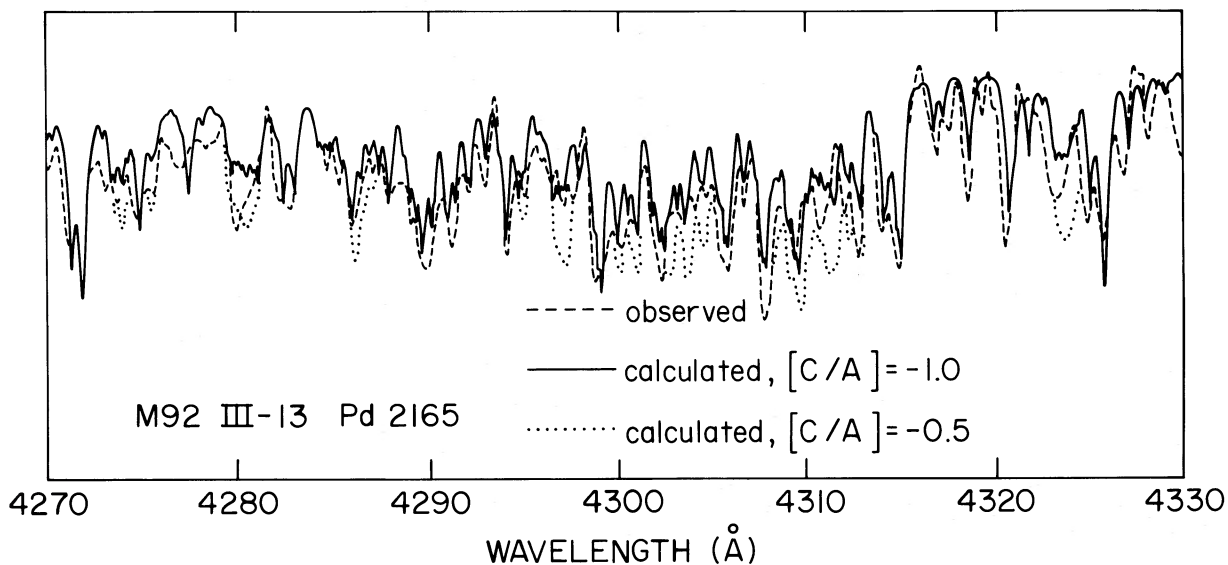


FIG. 6.—The spectrum of plate Pd 2165 of the M92 star III-13, in the wavelength region  $4270\text{--}4330 \text{ \AA}$ , is compared with model spectra computed for  $[C/A] = -0.5$  and  $-1.0$ .



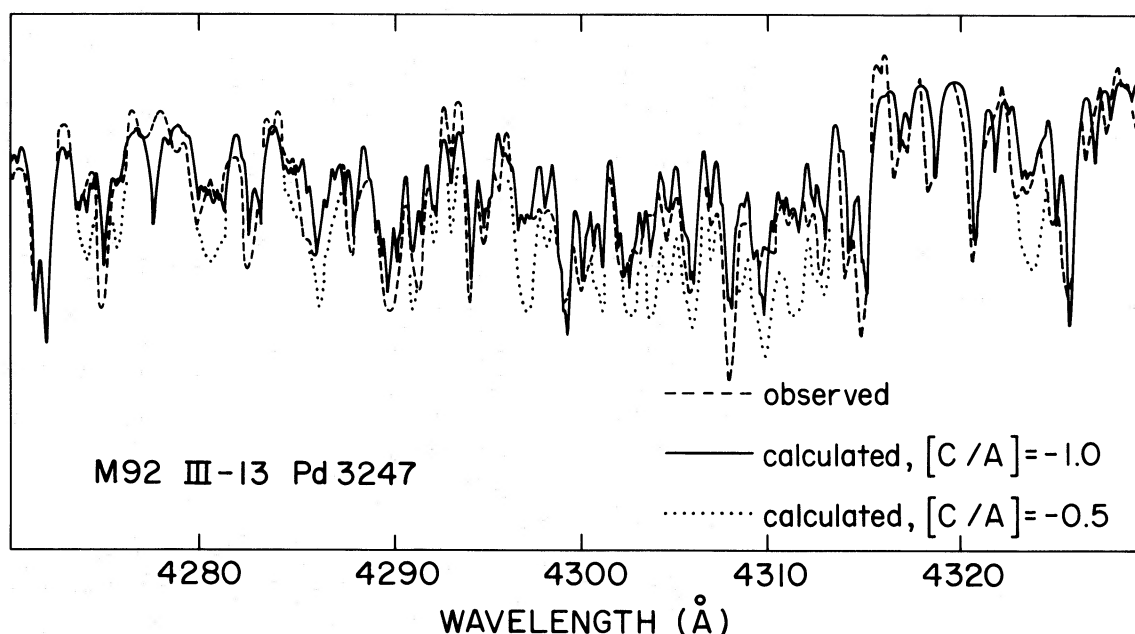


FIG. 7.—As Fig. 6 except that the observed spectrum is plate Pd 3247

results when analyzing stellar spectra, it is also apparent that firm conclusions about carbon weakness can still be drawn. In particular, a low DBV cannot be the cause of the low carbon abundances found. The reason is that the value of  $2 \text{ km s}^{-1}$  used in the work presented here cannot sensibly be reduced much further.

The synthetic spectra used for the atlas can also be used in color calculations to indicate the potential for

detecting weak G band stars photometrically and determining their carbon abundances. These colors will be discussed in the next section.

In Figures 6–13 we show the observed spectra for our stars and the corresponding calculated spectra. Since the continuum level of each observed spectrum is unknown, when comparing observed and calculated spectra we are forced to determine the intensity scale

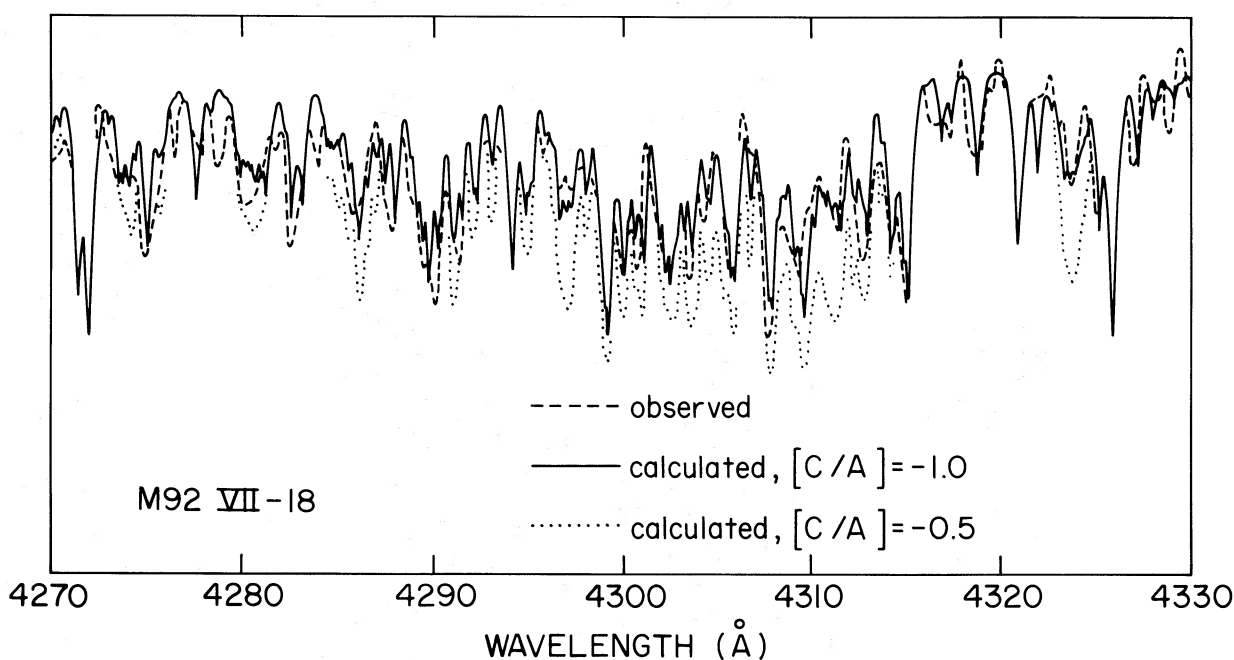


FIG. 8.—As Fig. 6 except that plate Pd 962 of the M92 star VII-18 is shown

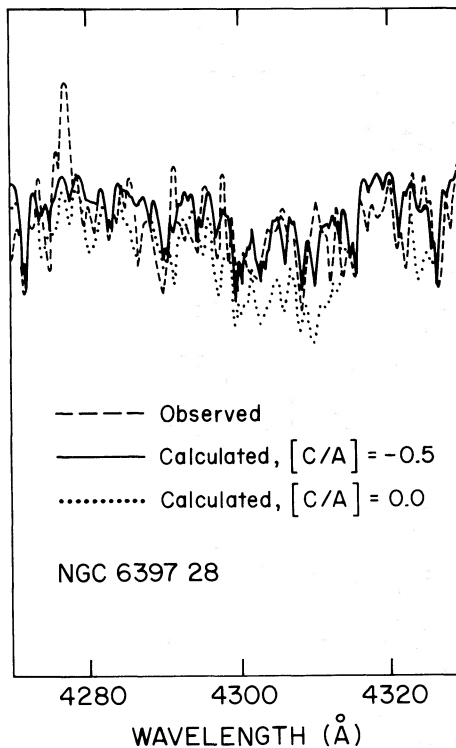


FIG. 9.—The observed spectrum of the star NGC 6397 28 is compared with model spectra computed for  $[C/A] = 0.0$  and  $-0.5$ .

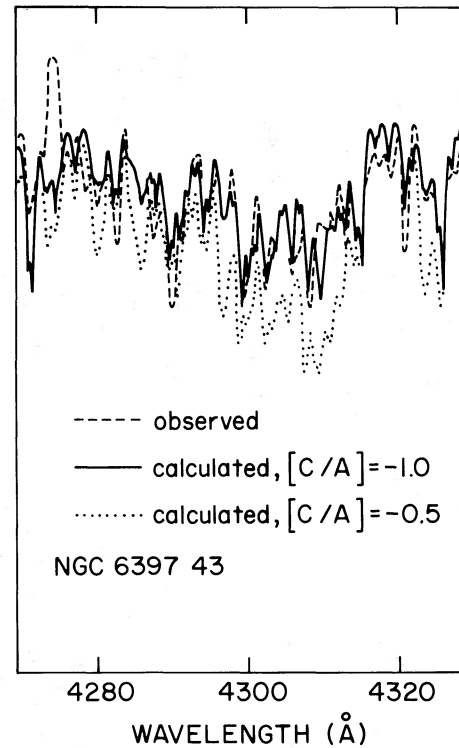


FIG. 10.—The observed spectrum of the star NGC 6397 43 is compared with model spectra computed for  $[C/A] = -0.5$  and  $-1.0$ .

of the calculations by fitting them to the tracings of the observed spectra in regions where the line absorption is relatively weak. For the present project we have chosen to do this fitting at wavelengths of 4220 Å and 4320 Å. The values found for the carbon abundances should not be very sensitive to the continuum levels adopted for the stars analyzed here. The CH features are not so weak that their strengths are materially altered by changes in continuum level;

furthermore, the strengths of CH features are essentially being estimated relative to the strengths of atomic lines. In order to avoid cluttering the diagrams, in most cases only calculated spectra for  $[C/A] = -0.5$  and  $-1.0$  are shown. The value of  $DBV = 2 \text{ km s}^{-1}$  in all cases. Comments on the individual stars are given below, beginning with the M92 stars for which the data are of higher quality. The deduced values of  $[C/A]$  are collected in Table 2.

TABLE 2  
[C/A] ABUNDANCES FROM INDIVIDUAL CARBON FEATURES

STAR No.	PLATE* OR FILM† No.	INTERVAL (Å)							MEAN [C/A]	REF. FIG. No.
		4273– 4275	4280– 4282	4285– 4287	4296– 4298	4303– 4305	4310– 4313	4322– 4324		
M92:										
III-13.....	Pd 2165	-0.6	-0.5	-1.0	-1.0	-1.0	-1.0	-0.7	-0.8	6
III-13.....	Pd 3247	-1.0	-1.0	-0.8	-1.0	-1.0	-1.0	-0.9	-1.0	7
VII-18.....	Pd 962	-0.7	-0.7	-0.9	-1.2	-1.0	-1.0	-1.2	-1.0	8
NGC 6397:										
28.....	853 M2 B	...	≤0.5	≤0.5	≤0.5	≤0.5	≤0.5	≤0.5	≤0.5	9
43.....	852 M2 B	...	-0.9	-1.0	-1.0	-1.0	-1.0	-1.0	-1.0	10
603.....	852 M2 A	...	-0.7	-1.0	-0.9	-0.9	-1.2	-0.9	-0.9	12
603.....	875 M3 E	...	-0.7	-0.7	-0.9	-1.0	-1.0	-1.0	-0.9	11
211.....	851 M2 A	...	-0.9	-0.7	-1.0	-0.9	-0.7	-1.0	-0.9	13

\* Pd—Palomar coudé, 18 Å mm<sup>-1</sup>.

† M2, Radcliffe spectracon, 50 Å mm<sup>-1</sup>; M3, Radcliffe spectracon, 22.5 Å mm<sup>-1</sup>.

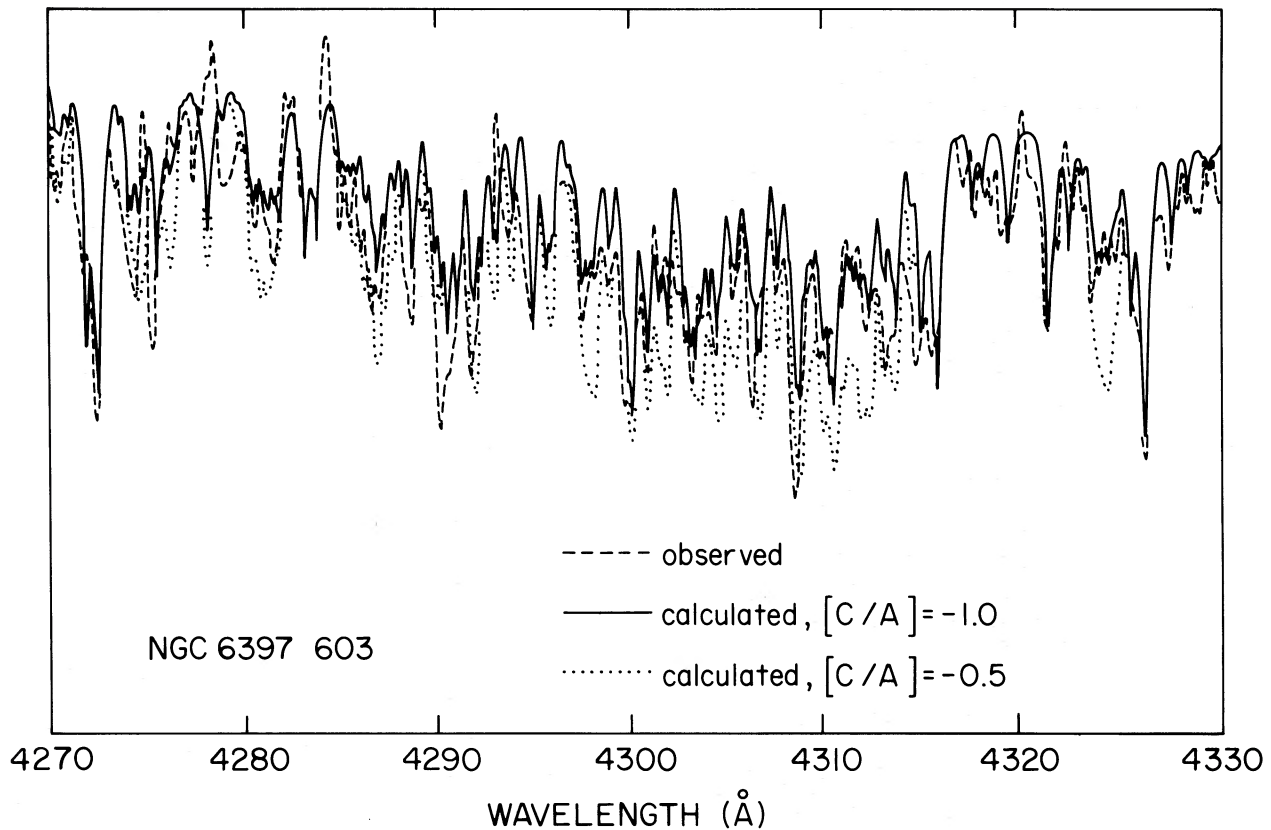


FIG. 11.—As Fig. 10, the observed spectrum being a  $22.5 \text{ \AA mm}^{-1}$  spectrum of NGC 6397 603

i) M92 III-13. Two spectra, Pd 2165 and Pd 3247, are available for this object. The 4300 and 4323 Å regions immediately show that the assumptions and techniques used lead to  $[C/A] \leq -0.5$  in Figures 6 and 7. Plate Pd 2165 gives a carbon depletion of  $[C/A] = -0.8$ , individual values being between  $-0.5$  and  $-1.0$ . For plate Pd 3247, the average  $[C/A]$  for the seven selected regions is  $-1.0$ , with the individual values lying between  $-0.8$  and  $-1.0$ . The mean value of  $[C/A] = -0.9$  is adopted for the star.

ii) M92 VII-18. The effective temperature of 4200 K causes the CH lines to be sensitive indicators of  $[C/A]$ . Inspection of Figure 8 in the wavelength region 4295–4315 Å and at 4323 Å shows that the procedures used must lead to  $[C/A]$  being less than  $-0.5$ . Comparison of observed and calculated spectra in the seven selected wavelength regions yields a mean  $[C/A] = -1.0$ , the individual fits ranging between  $-0.7$  and  $-1.0$ .

iii) The star NGC 6397 28 is the hottest star in the sample, and the CH features are consequently intrinsically weaker. For that reason, in Figure 9 the observed spectrum is compared with spectra computed for  $[C/A] = 0.0$  and  $-0.5$ . The CH lines in the former case are certainly too strong. It is difficult to adopt a specific  $[C/A]$  value from the general fit of the spectrum in the CH sensitive regions. The best course appears to be to adopt  $[C/A] \leq -0.5$ .

iv) Since NGC 6397 43 has  $T_{\text{eff}} = 4600 \text{ K}$ , the CH

lines are again good indicators of  $[C/A]$ . The CH sensitive regions give  $[C/A] = -1.0$ , with very little scatter (cf. Fig. 10).

v) Two spectra are available for NGC 6397 603, at dispersions of 50 and  $22.5 \text{ \AA mm}^{-1}$ . The higher-dispersion spectrum gives an average value of  $[C/A] = -0.9$ , the range being  $-0.7$  to  $-1.0$  (Fig. 11), and the lower-dispersion one gives an average value of  $-0.8$ , the range being  $-0.7$  to  $-1.2$  (Fig. 12). The agreement is gratifying.

vi) The star NGC 6397 211 has a mean  $[C/A] = -0.9$ , with the values given by the individual CH sensitive regions varying between  $-0.7$  and  $-1.0$  (cf. Fig. 13).

It is worth pointing out that reduction of  $[C/A]$  to  $-1.5$  causes visible differences in the computed spectra at  $T_{\text{eff}} = 4600$  and  $4250 \text{ K}$  (but not at  $5000 \text{ K}$ ). It appears that this low carbon abundance can be excluded for all our stars except NGC 6397 28.

We have estimated the effects of a change in the overall chemical compositions of the stars on the derived carbon abundances using model spectra computed for  $[A/H] = -3.0$ . We conclude that if  $[A/H]$  were  $-2.5$  instead of  $-2.0$ , the depletion values in column (10) of Table 2 would not be as great, the alteration being about 0.2 to 0.3 dex. It is clear that for any reasonable value of the overall metal abundance of the stars, the carbon is substantially depleted

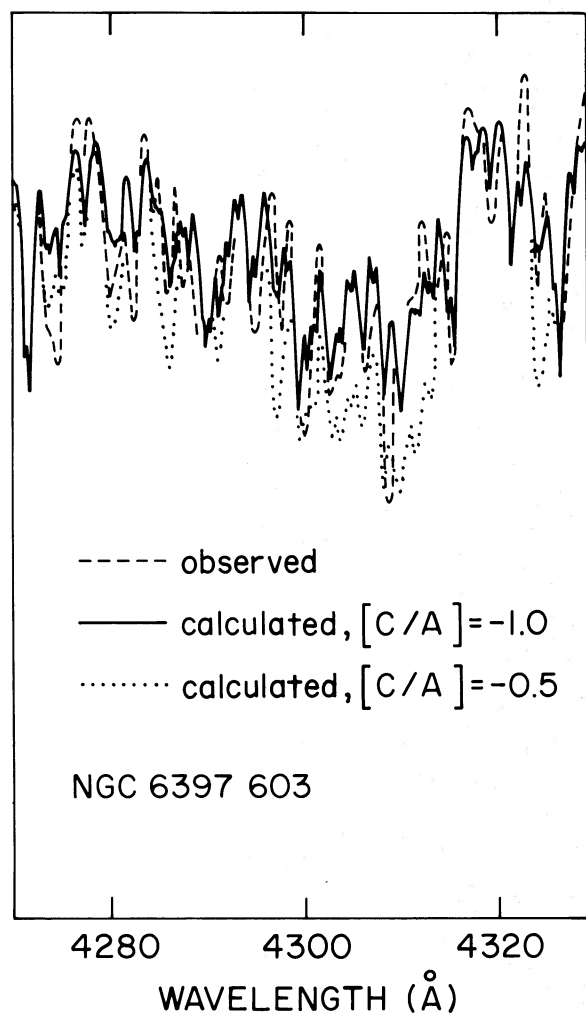


FIG. 12.—As Fig. 11, the observed spectrum being a  $50 \text{ \AA mm}^{-1}$  spectrum of NGC 6397 603.

relative to the other metals. A depletion of 0.7 dex is the more probable value for the M92 stars, with their lower metal abundances, whereas 1.0 is appropriate for NGC 6397.

The carbon depletion raises the possibility that the  $^{12}\text{C}/^{13}\text{C}$  ratio may be much less than the solar value of 89, a point which has been made on theoretical grounds by Mengel and Sweigart (1977). Krupp (1974) has computed wavelengths for  $^{13}\text{CH}$  lines and has identified such lines in the spectrum of Arcturus. Synthetic spectra were computed for the model 4250/0.75/-2.0, using  $^{12}\text{C}/^{13}\text{C} = 4$  and 89. In order to obtain maximum accuracy in the comparison, a step size of  $0.02 \text{ \AA}$  was used in the spectrum calculations. The differences between the spectra in the wavelength region 4250–4350  $\text{\AA}$  are unfortunately too small to be detected, even with the excellent observational material at our disposal. A resolution of better than  $0.1 \text{ \AA}$  would be required in order to usefully be able to study  $^{13}\text{CH}$ .

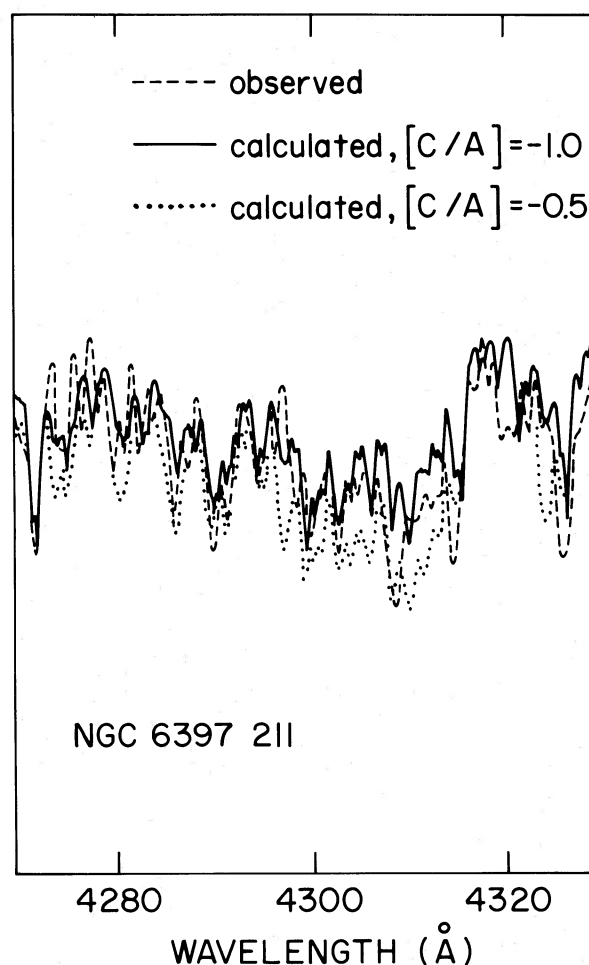


FIG. 13.—As Fig. 12, the observed spectrum being that of the star NGC 6397 211.

Calculations of the 4100–4215  $\text{\AA}$  region, using  $[\text{C}/\text{A}] = -1.0$  and  $[\text{N}/\text{A}] = +1.5$ , showed only minuscule enhancement of CN features when compared with the standard case with  $[\text{N}/\text{A}] = 0.0$ . Our spectroscopic material therefore does not allow confirmation of the results of Carbon *et al.* (1977) that  $[\text{N}/\text{A}] = +1.0$  for the M92 stars III-13 and VII-18 and we are unable to comment on the nitrogen abundance in the NGC 6397 stars.

Since carbon is depleted by CO formation, it is of interest to see if a large overabundance of oxygen will produce significant weakening of the CH lines. Calculations using the model 4250/0.75/-2.0 show that oxygen and carbon abundances of  $[\text{O}/\text{A}] = +1.0$  and  $[\text{C}/\text{A}] = 0.0$  produce a spectrum in which the CH lines are still stronger than is the case with  $[\text{C}/\text{A}] = -0.5$ ,  $[\text{O}/\text{A}] = 0.0$ , the oxygen-rich case corresponding to  $[\text{C}/\text{A}] \approx -0.3$  in the carbon-poor case. The weakness of the CH lines observed in our stars consequently cannot be caused by an oxygen overabundance of this amount. Moreover, an enhanced oxygen abundance would be inconsistent with the observed CO strengths. The actual value of the carbon abundance

does depend on the oxygen abundance, but this leads to uncertainties in  $[C/A]$  which are much smaller than the carbon depletion found.

It should be noted that, while the stars in our sample all show similar carbon depletions, there is still a considerable range in G band strength along the cluster giant branches, a point shown clearly in Figure 4. This makes it difficult, if not impossible, to relate visual estimates of G band strengths to carbon depletions, without supporting theoretical spectra. For example, Norris and Zinn (1977) have commented on G band strengths of stars in M13, M92, NGC 6397, and M15, on the basis of low-dispersion spectra of samples of stars in each cluster. Both M92 III-13 and VII-18 are described as having "strong" G bands whereas, as shown earlier, the G bands in these objects imply a very low carbon abundance. Similarly, NGC 6397 28 and 43 are described as having "weak" G bands while NGC 6397 603 and 211 are described as "strong." The G bands in three of these four stars yield  $[C/A] = -1.0$ , and NGC 6397 28 has  $[C/A] \leq -0.5$ . The main difference in the appearance of the spectra is due to the higher temperatures of the stars NGC 6397 28 and 43.

Mallia (1977) has discussed the spectroscopic properties of a number of stars in NGC 6397, including the stars 28, 43, 211, and 603. He quotes a carbon depletion for NGC 6397 28 as being between 20 and 40, and for NGC 6397 43 he implies an underabundance of a factor of 10, in addition to giving carbon depletions for a number of other stars. The very low carbon abundance found for NGC 6397 28 appears to be predominantly caused by the fact that Mallia uses a stellar temperature which is 300 K too low and, in general, his stellar temperatures are too low by 200 K or more.

Examination of the spectra published by Mallia, by Norris and Zinn, and our own low-dispersion material enable approximate estimates of the carbon abundances by direct interpolation in our atlas of stellar spectra (Fig. 4). It is of particular interest to see if carbon depletion occurs further down the subgiant branch. From Figure 2 of Mallia (1977) it is clear that the AGB star NGC 6397 75, having a similar temperature (5000 K) to 28, also has a similar carbon depletion whereas the subgiant NGC 6397 685, which has essentially the same temperature, has a G band strength indicating a close to normal carbon abundance (see Fig. 4 for models of  $T_{\text{eff}} = 5000$  K). The lower giant branch stars in NGC 6397 studied by Norris and Zinn are all denoted "strong G band," and a comparison of the spectra of such stars as 686 and our own spectra of 608 (see Fig. 14) with the model spectra clearly show carbon abundances close to normal. Taken together, the spectroscopic data therefore suggest substantial depletion of carbon for AGB stars and the brighter giants, close to a factor of 10 underabundance, whereas stars on the lower giant branch appear to have normal abundances, i.e.,  $[C/A] = 0$ . The fact that the star NGC 6397 685 has such a normal abundance suggests the carbon depletion sets in brighter than about  $M_v = -0.5$ . We shall return to this point in the discussion of the photometry.

The effects of departures from LTE, and the departures from the assumption of plane-parallel stratification, must now be examined. We shall first restrict the discussion to the direct effects on formation of CH lines and later comment on the more indirect effects through the model atmospheres. It is not possible at present to make a rigorous study of the effects of departures from LTE on the equivalent widths of the CH lines in late-type stars, since the relevant physical data, such as collision cross sections, are generally not available. Also, the computational difficulties are considerable. However, some estimates of the maximum effect have been made, assuming that all collisional effects on the electronic transitions may be disregarded, and that the molecule in this respect may be approximated by a system with two bound levels and a continuum. The simple representation of the complex molecular structure by a two-level system should be reasonable for the  $\Delta v = 0$  sequence of CH in late-type giants (cf. Hinkle and Lambert 1975).

The only transitions connected with the continuum which have been considered (i.e., processes which destroy and create molecules) were photodissociation and photoassociation, with predissociations via the  $C^2\Sigma^+ - X^2\Pi$ ,  $B^2\Sigma^- - X^2\Pi$  and  $A^2\Delta - X^2\Pi$  transitions. Only the first two, caused by the radiation from the wavelength interval  $2500 \text{ \AA} < \lambda < 3000 \text{ \AA}$ , were found to be important. Self-absorption in these transitions was not considered, so the departures from LTE are considerably exaggerated. The ultraviolet mean intensities were estimated from the fluxes of our model atmospheres. The relevant cross sections were taken from Solomon and Klemperer (1972) but the exact values of these data are not very important as long as the other transitions are totally disregarded.

The resulting effects on the dissociation equilibrium of CH, which certainly are overestimates, are rather great in the outer layers of the metal-poor models. For example, for the model 4500/1.5/-2.0 we obtain  $N_{\text{CH}}^{\text{NLTE}}/N_{\text{CH}}^{\text{LTE}} = 0.15, 0.31, 0.65,$  and  $1.0$  at  $\log \tau_{4300} = -3, -2, -1,$  and  $\geq -0.6$ , respectively. In other words, if LTE is assumed,  $[C/H]$  is underestimated by about 0.2. For the more metal-rich models, the effects are considerably smaller, since the strong ultraviolet blocking leads to a thermalized radiation field.

The abundance of CH molecules is dependent of the dissociation equilibrium of CO, which might also be affected by departures from LTE similar to those discussed above for CH. However, these departures are probably small and therefore unimportant at the depths where the CH lines are formed. The reason for this is that the dissociation energy of CO is so high that the ultraviolet radiation needed to photodissociate this molecule is well thermalized, even near the surface of the atmospheres.

Since collisions are neglected, the spectral lines are formed completely by scattering processes, and their weakening due to departures from the Boltzmann distribution (which are caused by the fact that the source function is considerably greater than the Planck field with the local temperature) is dependent

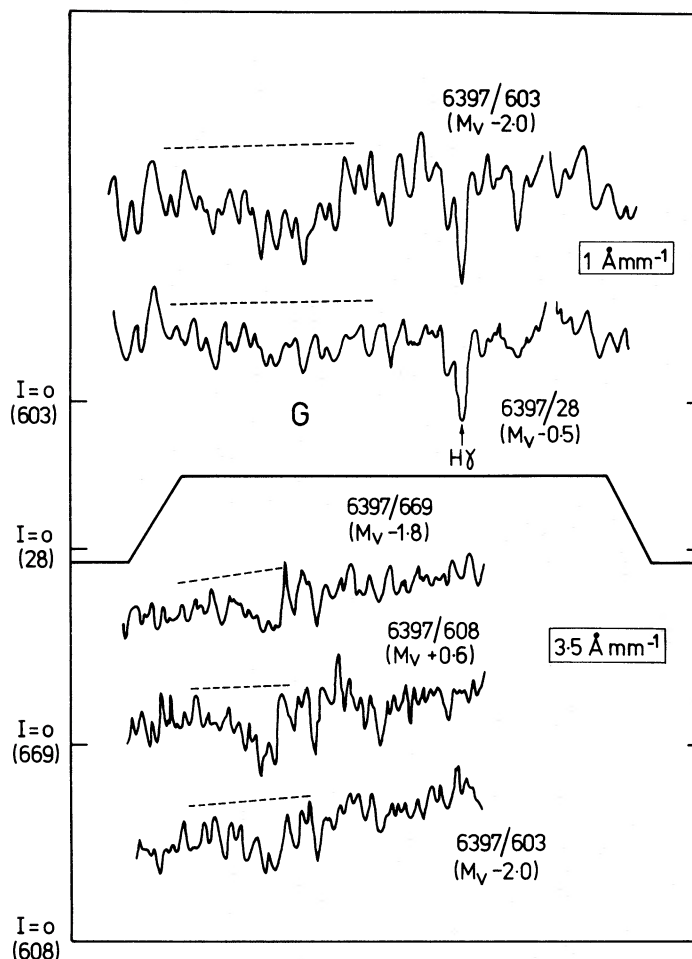


FIG. 14.—Comparison of spectra of several stars in NGC 6397 to illustrate the “normal” appearance of the G band in star 608. The upper panel shows the weakness of the G band of NGC 6397 28 compared to the brighter giant, 603. The latter star is compared at lower dispersion in the lower panel to another bright giant (669) and 608, which is seen to have quite comparable G-band strength to that of the bright giants.

only on the strength of the lines. Corrections to the LTE abundance determinations from single CH lines due to scattering effects have been found to be no more than 0.2 in  $[C/A]$  for the present models.

For single lines, we thus find that the estimated non-LTE (NLTE) effects, due to photodissociation and scattering effects, are quite small, corresponding only to an observable CH abundance change of  $[CH^{NLTE}/CH^{LTE}] \approx -0.4$ . However, for the reasons given above, this should be an overestimate of the effects. Moreover, the fact that many CH lines tend to overlap should diminish the NLTE effect further, since the source function will generally decrease due to this overlap. Thus, on the basis of this preliminary study we conclude that the large carbon deficiencies found in the present paper cannot be explained as a result of departures from LTE of the CH molecules. These effects probably contribute rather little to the CH line-weakening.

One might ask whether the carbon depletion effect could be the result of more indirect departures from LTE, affecting the structures of the stellar atmospheres themselves. The contribution function for the CH lines peak sharply toward the deeper layers of the atmospheres ( $\tau_{4300} > 0.03$ ), where the main opacity contributor,  $H^-$ , is definitely formed in LTE (cf. Gustafsson and Bell 1978). However, the electron donors, particularly iron, might be more ionized than the Saha equation predicts, as a consequence of the transparency of the metal-poor atmospheres in the ultraviolet and the fact that the dominant opacity source at these wavelengths is the Rayleigh scattering of H I, which allows the hot radiation from below to reach the upper layers. This extra photoionization would increase the continuum  $H^-$  opacity somewhat, and thus decrease the strength of the CH lines. However, this would not lead to the great effects observed for the G band; moreover, the Fe I lines would be still

more affected, such that the C/Fe ratio in an LTE analysis would be more likely to increase than to decrease.

The surface cooling, caused by blanketing due to metals and CO molecules, may well be considerably less than the LTE models predict, since many of the spectral lines are formed by scattering processes rather than by pure absorption. However, the CH line strengths do not change appreciably if the surface cooling is reduced, since the lines are formed at rather great depths.

Finally, it should be noted that the errors arising from the assumption of plane-parallelism of the model atmospheres are probably unimportant. The continuum colors, used in the temperature determination, and the CH bands are formed in roughly the same relatively deep layers, which means that sphericity effects are probably unimportant (cf. Gustafsson and Bell 1978). Inhomogeneities could, however, be significant. For example, if an atmosphere is postulated to consist of one component with  $T_{\text{eff}} = 4000$  K and one with  $T_{\text{eff}} = 5000$  K, both giving equal brightness at 4500 Å and with  $[A/H] = -2$  and  $[C/A] = 0.0$ , then this would erroneously be assumed to be a star with  $T_{\text{eff}} \approx 4500$  K and  $[C/A] \approx -0.5$  in the present analysis, since the strength of the CH band peaks at  $T_{\text{eff}} \approx 4500$  K. Such great temperature inhomogeneities in Population II giants cannot be completely disregarded (cf. Gustafsson and Bell 1978). However, the evidence for their existence is quite weak, and they would cause significantly smaller depletions for stars with hotter and cooler effective temperatures, which is not observed. Moreover, the infrared CO observations also suggest a considerable carbon depletion, which would not be expected from such an inhomogeneous atmosphere.

The possibility of weak G band stars being optical doubles can be dismissed using similar arguments, as well as the fact that such doubles would be well above the giant branch, which is not observed to be the case for weak G band stars. The possibility of emission from an extended atmosphere causing a veiling of the spectrum in the G band region may be dismissed, since this effect would cause a weakening of Fe I and other lines which is not observed. It would also affect the continuum colors and thus cause systematic differences in effective temperature determinations from different colors, which are not found.

Finally, the influence of effective temperature errors on the final results can be estimated from Figure 4. For example, a temperature change of 100 K should produce a change of only  $\sim 0.1$  in  $[C/A]$  at 4500 K and 0.15 at 5000 K. The effects of plausible errors in surface gravity will be small.

#### IV. ANALYSIS OF THE PHOTOMETRIC DATA

In order to obtain results for a larger sample of stars, and to look for confirmation of our spectroscopic results, it is of interest to investigate the photometric consequences of the low carbon abundances in the globular cluster giants. Calculations have been carried out for the 1.9–2.5  $\mu\text{m}$  region and the 3500–4350 Å region.

We have calculated synthetic spectra for the wavelength region of the first overtone bands of CO, using CO line data supplied by Kunde, the details of the wavelength and line-strength calculations being given by Kunde (1970). The relatively coarse step size of 1.0 Å was found to be adequate. Allowance has been made for the effect of terrestrial atmospheric absorption in the color calculations (cf. Bell, Dickens, and Gustafsson 1978). The CO color, 2.20 – 2.36 on the Cohen, Frogel, and Persson (1978) system, showed the expected variation with metal abundance and carbon abundance. The colors found are as follows, with the normalization being carried out using a Vega model in the same way that the observers use Vega: 4250/1.50/0.0, CO = +0.12 mag; 4250/0.75/–2.0, CO = +0.07 mag; 4250/0.75/–2.0 and  $[C/A] = -1.0$ , CO = +0.02 mag. Cohen, Frogel, and Persson find the CO colors for M92 III-13 and VII-18 to be 0.01 and –0.02 mag, respectively, and the mean CO index for an M67 star of the same V – K color as the M92 stars is 0.12. The CO color difference between the M67 and M92 stars thus requires that the carbon abundance be very low in the M92 stars, confirming the result from the CH lines.

It is apparent that various photometric systems could be used to search for carbon deficient stars. For example, the Uppsala system (Häggkvist and Oja 1970) and the Brorfelde system (Dickow *et al.* 1970) would be quite suitable. Since, however, almost all the existing observations of stars in globular clusters have been made using the DDO system, we consider only this system in the present paper.

TABLE 3  
CHANGES IN CALCULATED 41 AND 42 MAGNITUDES OF THE DDO SYSTEM RESULTING FROM CHANGES IN CARBON ABUNDANCE

Model	$\Delta C41$	$\Delta C41$	$\Delta C42$	$\Delta C42$
	$[C/A] = -0.5$	$[C/A] = -1.0$	$[C/A] = -0.5$	$[C/A] = -1.0$
5500/3.0/–2.0 . . . .	–0.003	–0.004	–0.015	–0.020
5000/2.25/–2.0 . . . .	–0.013	–0.017	–0.054	–0.078
4500/1.5/–2.0 . . . .	–0.036	–0.052	–0.087	–0.145
4000/0.75/–2.0 . . . .	–0.050	–0.068	–0.080	–0.128
3750/0.75/–2.0 . . . .	–0.039	–0.052	–0.058	–0.088

In Table 3 we give the changes in the 41 and 42 magnitudes of the DDO system brought about by changes of  $[C/A]$  equal to  $-0.5$  and  $-1.0$ . The nitrogen abundance has been kept fixed at  $[N/A] = 0.0$ ; but since CN cannot be detected in the spectrum of the 4250/0.75/-2.0 model even if  $[N/A] = +1.0$ , it is very unlikely to affect the 41 magnitude. The color changes resulting from the  $[C/A]$  changes are substantial by photometric standards.

The  $C(45 - 48)$ ,  $C(42 - 45)$  diagram is shown for M92 and NGC 6397 in Figure 15, the data sources being given above. The values of  $T_{\text{eff}}$  and  $\log g$  along the NGC 6397 giant branch (from Fig. 2) and the theoretical colors of Bell and Gustafsson (1978) are used to draw the standard giant branch line for  $[A/H] = -2.0$ . When drawing this line, it has been necessary for us to use colors computed under the assumption that the abundances of all elements vary in unison and that the DBV =  $2 \text{ km s}^{-1}$ . Since the 45 and 48 magnitudes are essentially unaffected by carbon abundance changes, the alterations produced in the 42 magnitude can be used to find the anticipated giant branch lines for different  $[C/A]$ . Figure 15 shows that the brighter giant stars in the two clusters; i.e., M92 III-13, VII-18, V-45, and XII-8, and NGC 6397 211, 669, and 43 are all carbon-poor. The carbon deficiencies derived from the photometry are not quite as large as those found spectroscopically. If we had used a higher DBV when finding the colors of the 4000 K model, the carbon deficiencies found photometrically would be increased, becoming closer to the spectroscopic values. This comes about because increases in DBV make colors become redder, with the effect on  $C(42 - 45)$  being substantially greater

than on  $C(45 - 48)$ . The  $C(45 - 48)$  color of XII-8 again indicates  $T_{\text{eff}} = 4450 \text{ K}$ , confirming our temperature scale.

Figure 15 also shows that the fainter NGC 6397 stars and the fainter M92 stars, viz., II-6, III-4, IV-2, IV-10, IV-114, and VI-18, lie very close to the standard line. However, the faintest star observed in M92, viz., III-81, is very close to the  $[C/A] = -1.0$  line. This is probably caused by a shift in  $C(45 - 48)$  due to its substantially lower gravity as compared to subgiant stars of a similar color and so it is presumably carbon deficient.

The photometry therefore suggests that the carbon depletion in the other cooler stars occurs as the stars evolve up the giant branch, with the effect beginning near  $M_v = -0.7$ . The stars which are brighter than this all show a carbon deficiency. Furthermore, those in a later evolutionary stage such as the AGB star NGC 6397 28 also have carbon depletions according to the spectroscopic analysis. Both this star and another probable AGB star we have analyzed in M92 (XII-34), which has  $[C/A]$  close to  $-1$ , would be expected to lie near the  $[C/A] = -1$  line in Figure 15. It would be interesting to check this from DDO colors for these two stars. Spectroscopic evidence for stars with  $M_v > -0.7$  having normal G bands is given earlier. Carbon *et al.* (1977) in their discussion of carbon abundances in M92 stars find, as a preliminary result, that the carbon depletion begins in some stars at a fainter  $M_v$ , viz.,  $+1.0$ .

The photometric data and corresponding calculations for the  $C(41 - 42)$ ,  $C(42 - 45)$  diagram are shown in Figure 16. Since the 41 magnitude is affected by CH, and possibly by CN, it is affected by the carbon

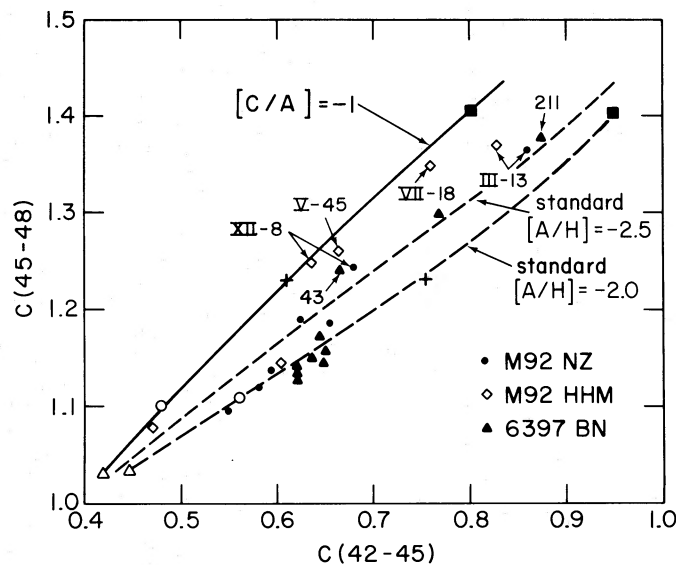


FIG. 15.—The  $[C_0(45 - 48)$ ,  $C_0(42 - 45)]$ -diagram for NGC 6397 and M92. The sources of stellar data are: NZ = Norris and Zinn (1977); HHM = Hesser, Hartwick, and McClure (1977); BN = Bessell and Norris (1978). Individual stars are identified. The standard line for  $[A/H] = -2.0$  is that computed from the  $T_{\text{eff}}$ ,  $\log g$  of the mean giant branch of the cluster NGC 6397, the colors corresponding to  $T_{\text{eff}} = 4000, 4500, 5000$ , and  $5500 \text{ K}$  being identified by the symbols of Fig. 2. The standard line for  $[A/H] = -2.5$  is also shown, as is the line for  $[C/A] = -1$ ,  $[A/H] = -2.0$ .



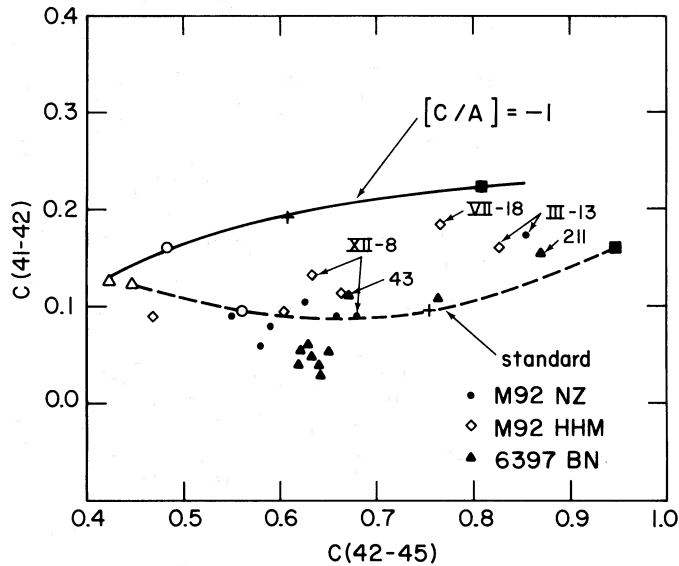


FIG. 16.—As Fig. 15, except that the colors are  $C_0(41 - 42)$  and  $C_0(42 - 45)$

changes. The stars which are displaced toward the carbon-deficient branch in Figure 15 are also displaced in Figure 16, although the displacement is again not quite as large as would be expected for the spectroscopic results. There is also a suggestion that the NGC 6397 stars are systematically displaced by about 0.05 mag in  $C(41 - 42)$  relative to the M92 stars. As mentioned above, the lines of the (0, 1) sequence of the violet CN system are too weak to be used to deduce nitrogen abundances.

Since the (0, 0) sequence of the violet CN system is much stronger than the (0, 1) sequence, calculations

were carried out to see if the  $C(38 - 42)$  colors could be used to deduce nitrogen abundances. The color changes resulting from  $[N/A]$  being increased from 0.0 to 1.0, with  $[C/A] = -1.0$ , were found to be only 0.02 mag at  $T_{\text{eff}} = 4000$  and 4500 K. The  $C(38 - 42)$  colors thus cannot be used to find  $[N/A]$  in these very metal-poor stars.

Since the slope of the standard line in the  $[C(45 - 48), C(42 - 45)]$ -diagram is relatively shallow, the conclusions about carbon weakness derived from analysis of the  $C(42 - 45)$  colors depend on the  $C(45 - 48)$  colors being measured very precisely. For this reason

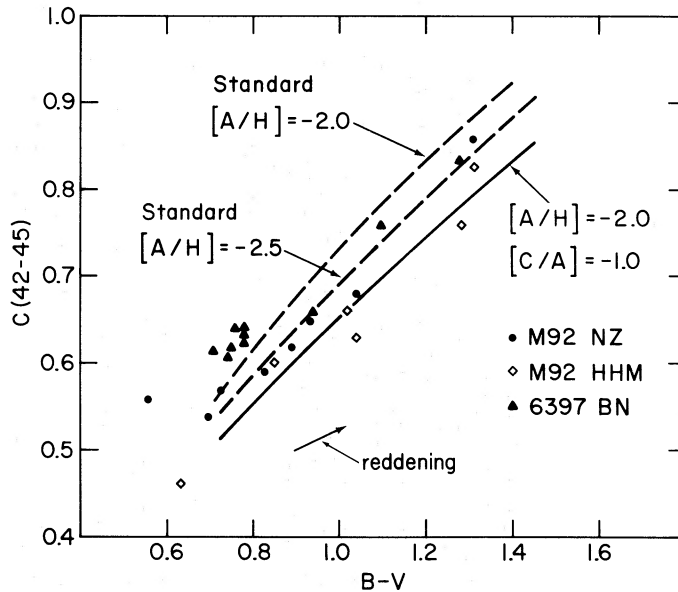


FIG. 17.—The  $[C_0(42 - 45), (B - V)_0]$ -diagram of M92 and NGC 6397 stars. The standard lines for  $[A/H] = -2.0$  and  $-2.5$  and the  $[C/H] = -1, [A/H] = -2.0$  line are shown. The reddening line is also shown.

we have checked the conclusions derived from the DDO diagrams by considering "hybrid" color-color diagrams.

CH lines contribute only a small fraction of the blocking in the passband of the  $B$  filter of the  $UBV$  system, and not at all in the  $V$  filter, so it seems that the  $B - V$  color of a globular cluster giant model should change by only 0.01 or 0.02 mag at the most when  $[C/A]$  is changed from 0 to  $-1.0$ . In these circumstances, a diagram of  $C(42 - 45)$  versus  $B - V$  should show the same behavior as the  $[C(42 - 45), C(45 - 48)]$ -diagram. On the other hand, the  $[C(45 - 48), B - V]$ -diagram should show very little scatter at all, since both colors are insensitive to carbon changes.

The  $[C(42 - 45), B - V]$ -diagram is shown as Figure 17. The standard lines for  $[A/H] = -2.0$  and  $-2.5$  are marked, together with the line for  $[A/H] = -2.0$ ,  $[C/A] = -1.0$ . The differential carbon abundance effect is apparent in this diagram for both clusters, with the brighter stars being displaced to lower carbon abundances relative to the fainter stars. The magnitude of the shift is as large as, or even slightly larger than, the effect found spectroscopically for M92 III-13 and VII-18. The NGC 6397 stars are slightly displaced relative to their anticipated positions. A zero-point shift would compensate for this, and the carbon abundances of NGC 6397 43 and 211 could then agree with the spectroscopic values for the case of  $[A/H] = -2.0$ . We do not understand, however, the cause of such a zero-point shift. It is doubtful that it arises from errors in the  $B - V$  photometry owing to the size of the effect required, i.e., 0.08 mag. It is possible that small errors exist in the DDO photometry, but, as shown below, a similar shift is needed in the  $[C(45 - 48), B - V]$ -diagram. Reddening errors can be ruled out since the slope of the reddening line is nearly parallel to the standard lines (cf. Fig. 17).

The  $[C(45 - 48), B - V]$ -diagram is shown as Figure 18. It is apparent that the M92 stars follow the standard line very well. The slope of the NGC 6397 stars is in good agreement with calculation, but a zero point shift of 0.04 mag in  $C(45 - 48)$  is needed for the stars to fit the calculations. This cannot be explained by abundance effects. When considering this diagram, it is worth noting that the standard line has been drawn solely from model atmosphere and synthetic spectra calculations and the  $(M_v, B - V)$ -diagram, with the only introduction of observation into the color calculations being the use of  $\phi^2$  Ori as the zero-point star (see Bell and Gustafsson 1978).

The discussion given above has been in terms of the overall metal abundance in both clusters being taken as  $[A/H] = -2.0$ . The standard lines for  $[A/H] = -2.5$  are sketched in Figures 15 and 17. In Figure 18 the standard line for  $[A/H] = -2.5$  is virtually indistinguishable from that for  $[A/H] = -2.0$ . The effect of a reduction in the overall metal abundance is to reduce the carbon depletions found for the brighter stars, and the "normal" carbon abundances ( $[C/A] = 0$ ) found for the fainter stars change to slight overabundances. The original effect, that the carbon abundance in the brighter stars seems much less than in the fainter stars, consequently still exists.

#### V. CONCLUSIONS

We have found that both spectroscopic and photometric data available at present show a weakening in the G band strength for most stars along the upper giant branches in M92 and NGC 6397 when comparisons are made with synthetic spectra and colors of model atmospheres. The effect occurs even in the coolest stars at the tip of the giant branch. This weakening of the G band corresponds to a carbon depletion such that  $-0.5 > [C/A] > -1.0$ . The

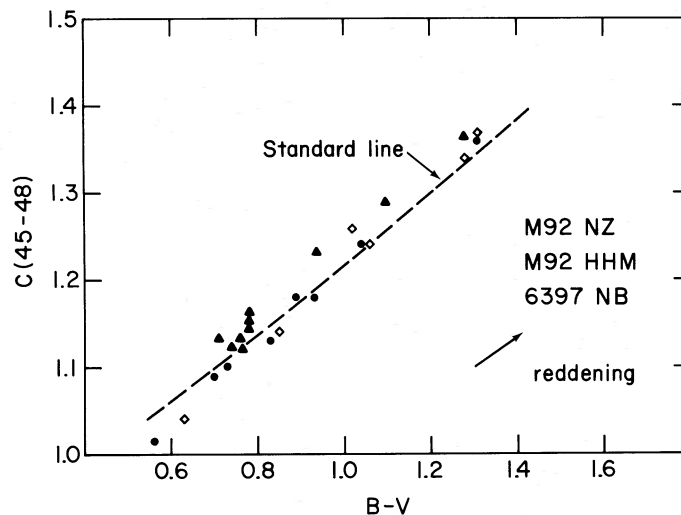


FIG. 18.—The  $C_0(45 - 48)$ ,  $(B - V)_0$  diagram of M92 and NGC 6397 stars, together with the standard line for  $[A/H] = -2.0$ . The reddening line is also shown.

photometric data on the  $2.4\ \mu\text{m}$  CO bands in two M92 stars confirm this conclusion. It is found that departures from LTE in the dissociation equilibrium of CH or in the source function of the lines are probably not responsible for the line weakening; instead it seems quite probable that it reflects a true abundance effect. Small improvements in these results could be made with better effective temperatures obtainable from more precise intrinsic colors. More significant improvements could result from increased accuracy in the determination of the overall metal abundance and the Doppler broadening velocity, and from higher-dispersion spectra and/or the use of well-calibrated very narrow band spectrophotometry (e.g., Gustafsson, Kjaergaard, and Andersen 1974) to measure specific CH features.

Some spectroscopic data suggest that this carbon depletion is less pronounced for stars on the lower giant branch, and the photometric DDO data indicate that the depletion vanishes for most stars with  $M_b > -0.7$ , which is in at least qualitative agreement with the hypothesis of deep meridional mixing of CNO processed material to the surface. It would certainly be very valuable to obtain independent higher-dispersion spectroscopic confirmation of the "normal" [C/A] values for stars on the lower giant branches of the metal-poor clusters. It would also be very valuable to obtain reliable nitrogen abundances, e.g., from the NH ultraviolet bands, for stars along the giant branches of these clusters, since the carbon depletion is probably the result of the CN cycle, converting carbon nuclei to nitrogen. This cannot yet be regarded as an established result, however, and further work aimed especially at establishing more definitely the origin of the abundance anomalies is needed. It would be of particular value to carry out a photometric DDO survey of globular cluster subgiant stars, followed by spectroscopic or very narrow band spectrophotometric investigation of "interesting" stars found from this photometry. Examples of interesting stars in this context might well be upper-giant-branch stars showing apparently normal C and N abundances and lower-giant-branch stars showing abundance anomalies. Should the latter be unambiguously identified as

cluster members, then origins other than those due to mixing must be considered.

Auer and Demarque (1977) have shown that a possible explanation of variations in the Balmer jump in blue horizontal branch stars in M92 is enhancements of C and/or N of between 100 and 1000 times. Such an enhancement is inconsistent with our results insofar as carbon is concerned, and the carbon depletions we observe would be expected to cause only modest enhancements of nitrogen.

One might ask whether this carbon depletion also shows up in the spectra of field giants of extreme Population II. In fact, the well-known very metal-poor star HD 122563 shows a carbon deficiency,  $[\text{C}/\text{Fe}] = -0.5$ , and a nitrogen enrichment,  $[\text{N}/\text{Fe}] = 1.2$  (Snedden 1973). Other low-gravity objects also show carbon deficiencies (Snedden 1974). We have also found that the two very metal poor giants HD 165195 and HD 221170 deviate in the  $C(42 - 45)$ ,  $C(45 - 48)$  diagram from their predicted locations (with stellar parameters adopted according to Gustafsson and Bell 1978), indicating carbon deficiencies. It would be very worthwhile to determine carbon and nitrogen abundances and  $^{12}\text{C}/^{13}\text{C}$  ratios for more field Population II giants, particularly those on the lower giant branch, by high-dispersion spectroscopy. Precise narrow-band (e.g., DDO) photometry for extensive samples of such stars would also be very valuable.

We are grateful to Drs. M. S. Bessell and J. E. Norris for sending their data in advance of publication and to the Hale Observatories for the generous loan of the Palomar spectrograms. Mr. J. Ohlmacher helped us with the programming, Mrs. E. Bingham, Mrs. I. Malin, and Dr. C. D. Pike with the reduction of the observations. Dr. B. Pagel made valuable comments on the manuscript and Dr. A. Sweigart kindly gave us a preprint. Dr. R. P. Kraft has kindly kept us informed of the extensive work of his group on M92. Some of the computations were carried out using the University of Maryland Computer Science Center. R. A. B. acknowledges support from the National Science Foundation.

#### REFERENCES

- Auer, L. H., and Demarque, P. 1977, *Ap. J.*, **216**, 791.  
 Bell, R. A., and Dickens, R. J. 1974, *M.N.R.A.S.*, **166**, 89.  
 Bell, R. A., Dickens, R. J., and Gustafsson, B. 1975, *Bull. AAS*, **7**, 535.  
 ———. 1978, "Symposium on Important Advances in 20th Century Astronomy," Copenhagen.  
 Bell, R. A., Eriksson, K., Gustafsson, B., and Nordlund, Å. 1976, *Astr. Ap. Suppl.*, **23**, 37.  
 Bell, R. A., and Gustafsson, B. 1978, *Astr. Ap. Suppl.*, **34**, 229.  
 Bessell, M. S., and Norris, J. E. 1976, *Ap. J.*, **208**, 369.  
 ———. 1978, private communication.  
 Bond, H. E. 1975, *Ap. J. (Letters)*, **202**, L47.  
 Brault, J., and Testerman, L. 1972, A Preliminary Edition of the Kitt Peak Solar Atlas, unpublished.  
 Butler, D. S. 1975, *Ap. J.*, **200**, 68.  
 Butler, D. S., Carbon, D., and Kraft, R. P. 1975, *Bull. AAS*, **7**, 239.  
 Cannon, R. D. 1974, *M.N.R.A.S.*, **167**, 551.  
 Carbon, D., Butler, D., Kraft, R. P., and Nocar, J. L. 1977, in *CNO Isotopes in Astrophysics*, ed. J. Audouze (Ap. Space Sci. Library, Vol. 67; Dordrecht: Reidel).  
 Christensen, C. G. 1972, Ph.D. thesis, California Institute of Technology.  
 Cohen, J. G., Frogel, J. A., and Persson, S. E. 1978, *Ap. J.*, **222**, 165.  
 Dickens, R. J. 1972, *M.N.R.A.S.*, **159**, 7p.  
 Dickens, R. J., and Bell, R. A. 1976, *Ap. J.*, **207**, 506.  
 Dickow, P., Gyldenkerne, K., Hansen, L., Jacobsen, P.-U., Johansen, K. T., Kjaergaard, P., and Olsen, E. H. 1970, *Astr. Ap. Suppl.*, **2**, 1.  
 Gingerich, O., Noyes, R. W., Kalkofen, W., and Cuny, Y. 1971, *Solar Phys.*, **18**, 347.  
 Grevesse, N., and Sauval, A. J. 1973, *Astr. Ap.*, **27**, 29.  
 Griffin, R. F. 1968, *A Photometric Atlas of the Spectrum of Arcturus,  $\lambda\lambda 3600-8825\ \text{\AA}$*  (Cambridge: Cambridge Philosophical Society).

- Gustafsson, B., and Bell, R. A. 1978, *Astr. Ap.*, in press.  
 Gustafsson, B., Bell, R. A., Eriksson, K., and Nordlund, Å. 1975, *Astr. Ap.*, **42**, 407.  
 Gustafsson, B., Kjaergaard, P., and Andersen, S. 1974, *Astr. Ap.*, **34**, 99.  
 Häggkvist, L., and Oja, T. 1970, *Astr. Ap. Suppl.*, **1**, 119.  
 Harding, G. A. 1964, *Observatory*, **82**, 205.  
 Helfer, H. L., Wallerstein, G., and Greenstein, J. L. 1959, *Ap. J.*, **129**, 700.  
 Hesser, J. E., Hartwick, F. D. A., and McClure, R. D. 1977, *Ap. J. Suppl.*, **33**, 471.  
 Hinkle, K., and Lambert, D. L. 1975, *M.N.R.A.S.*, **170**, 447.  
 Krupp, B. M. 1974, Ph.D. thesis, University of Maryland.  
 Kunde, V. G. 1970, NASA Tech. Report R-323.  
 Lambert, D. L. 1978, *M.N.R.A.S.*, **182**, 249.  
 Mallia, E. A. 1977, *Astr. Ap.*, **60**, 195.  
 Mengel, J., and Sweigart, A. 1977, *Bull. AAS*, **19**, 603.  
 Norris, J., and Zinn, R. 1977, *Ap. J.*, **215**, 74.  
 Sandage, A. 1970, *Ap. J.*, **162**, 841.  
 Sandage, A., and Walker, M. F. 1966, *Ap. J.*, **143**, 313.  
 Savitsky, A., and Golay, M. J. E. 1964, *J. Analyt. Chem. Wash.*, **36**, 1627.  
 Sneden, C. 1973, *Ap. J.*, **184**, 839.  
 ———. 1974, *Ap. J.*, **189**, 493.  
 Solomon, P. M., and Klemperer, W. 1972, *Ap. J.*, **178**, 389.  
 Sweigart, A. V., and Mengel, J. G. 1979, *Ap. J.*, **229**, 624.  
 Zinn, R. 1973, *Ap. J.*, **182**, 183.

R. A. BELL: Astronomy Program, University of Maryland, College Park, MD 20742

R. J. DICKENS: Royal Greenwich Observatory, Herstmonceux Castle, Hailsham, Sussex BN27 1RP, England

B. GUSTAFSSON: Astronomical Observatory, Box 515, S-751 20 Uppsala 1, Sweden